Photometric Redshifts and High Redshift Galaxies
ASP Conference Series, Vol. 191, 1999
R.J. Weymann, L.J. Storrie-Lombardi, M. Sawicki, and R.J. Brunner, eds.

The Nature of Small Galaxies in the Hubble Deep Field

Lisa J. Storrie-Lombardi & Ray J. Weymann

Observatories of the Carnegie Institution of Washington, 813 Santa Barbara Street, Pasadena, CA 91101

Rodger I. Thompson

Steward Observatory, The University of Arizona, Tucson, AZ 85721

Abstract. We present results from a study of very small galaxies (isophotal area $\leq 0.2^{\square''}$) with photometric redshifts $1 \leq z \leq 4.5$ detected in the region of the northern Hubble Deep Field covered by NICMOS observations at 1.6 and 1.1 microns. We estimate that $\sim$ 50 percent of these sources are star-forming galaxies at redshifts $2 < z < 3.5$ and $\sim$ 45 percent at are $3.5 < z < 4.5$, with the remaining 5% at $1 < z < 2$. We have examined averaged images of these faint ($V_{606} \sim 27$–29), compact objects to search for extended, surrounding flux from older, fainter populations of stars. We find no evidence that the small objects in the Hubble Deep Field are embedded in fainter, more extended galaxies. The majority are indeed isolated and compact. We estimate the 5σ depth of the averaged images to be $H_{160} \approx 29.8$ AB magnitudes per square arcsecond.

1. Introduction

The number counts, sizes, morphologies, and colors of galaxies are used to determine their evolutionary history and constrain cosmological models. It is therefore crucial to understand what we are counting and measuring as we peer deeper into the history of the Universe where objects appear fainter, smaller, and commonly measured features in rest frame optical wavebands move into the near-infrared and beyond. The optical images of the Hubble Deep Field (HDF) (Williams *et al.* 1996) showed us an exquisitely detailed view of some high redshift galaxies, though the view is inherently distorted (Ferguson 1998) due to the effects of cosmological surface brightness dimming, the effects of dust on galaxy colors, and the fact that we view higher redshift galaxies at progressively bluer rest wavelengths.

NICMOS observations of the Hubble Deep Field (Thompson et al. 1999) provide us with two additional redder wavebands to help disentangle some of these effects. For high redshift objects the combination of the brighter, clumpier star forming regions moving into the optical filters, and surface brightness dimming will make high redshift, compact, UV-bright objects more prominent than lower surface brightness objects at the same redshift (O'Connell & Marcum 1997). Colley *et al.* (1996) discussed how this is evident in the Hubble Deep

Field by measuring the two-point correlation function of galaxies detected in the WFPC2 fields. They found a positive signal in the correlation function for scales $\leq$ 1 arcseconds for small objects. At cosmological distances this corresponds to subgalactic scales, *e.g.,* 1 arcsecond $\approx$ 8 kpc for redshifts z > 1 (H_0 = 65 km s^{-1} Mpc^{-1}, q_0 = 0.125). This led them to suggest that many of the 'galaxies' detected by source counting algorithms are probably sub-galactic components.

NICMOS is better able to detect fainter, older stellar populations that might be connected with brighter star forming regions seen at bluer wavelengths, as well as galaxies whose radiation is extincted by dust at optical wavelengths. To better understand whether or not we are detecting galaxies or pieces of galaxies in the optical images, and how this might affect our interpretation of galaxy sizes and number counts versus magnitude, in this paper we explore the nature of compact sources detected Hubble Deep Field in the $\sim 0.65^{\square'}$ region covered by our NICMOS observations. We discuss below the selection of compact, high redshift sources from these data, and the examination of averaged images of compact galaxies, searching for evidence of diffuse, extended flux.

2. Selecting Compact, High Redshift Galaxies

The galaxies were selected with the SExtractor (Bertin & Arnouts 1996) software using all six available HST wavebands: F300W (U_{300}), F450W (B_{450}), F606W (V_{606}), F814W (I_{814}), F110W (J_{110}), and F160W (H_{160}). The technique is discussed in detail in Weymann, Thompson & Storrie-Lombardi (1999) and Storrie-Lombardi, Weymann, & Thompson (1999). The WFPC2 images were first transformed to the same orientation and scale as the NICMOS images, and then convolved with a Gaussian to match the broader NICMOS point spread function (PSF). The measured FWHM of the PSF is $\approx$ 0.2". Photometric redshifts were estimated for the 353 detected galaxies (Weymann *et al.* (1999).

For our sample of compact objects, we selected a subset (93 galaxies) that met the following criteria: (1) The isophotal area, as measured by SExtractor, is $\leq 0.2^{\square''}$. (2) The photometric redshift is $1.0 \leq z \leq 4.5$. (3) The SExtractor parameter FLAGS=0, so we only select objects that are not blended or overlapping with others. To test the robustness of the photometric redshifts determined for this sample we did simulations, perturbing the fluxes in each of the 6 wavebands, and then running the perturbed fluxes through the photometric redshift estimator. The value of σ to use for randomly adding noise to the measured fluxes was determined from the position of the detected galaxies using σ-maps made for each waveband (see Weymann *et al.* 1999). Each measured flux was randomly perturbed, using a Gaussian distribution and the 1σ flux determined from the map. Using this method we created 100 perturbed realizations for each detected galaxy, and then examined the photometric redshift distribution for each galaxy. We calculated the 10th and 90th percentile values for the redshift distribution (z_{10} and z_{90}) from the perturbed samples and compared these with the original photometric redshift estimates. Of the 93 galaxies in our sample, only 11 have z_{10} and z_{90} values within $\Delta z = 0.5$ of the value determined from the unperturbed fluxes. These are discussed in Storrie-Lombardi *et al.* (1999).

3. Averaging Images to Place Limits on Extended Flux

For the remaining galaxies, the photometric uncertainties are too large at these faint flux levels to obtain individual reliable photometric redshift estimates. To learn something about their mean properties and look for diffuse extended emission around the compact objects we have divided them by visual inspection into U_{300} drop-outs (23 galaxies) and B_{450} drop-outs (12 galaxies), selecting only those that appear not to have close companions. We then averaged together each waveband at the galaxy positions and used the fluxes measured from these images to obtain a 'mean' photometric redshift for each group. The U_{300} drop-out mean redshift is $z = 2.7$ and the B_{450} drop-out mean redshift is $z = 3.9$. All six HST wavebands for the U_{300} and B_{450} drop-outs are shown in figure 1. Overplotted are 0.6 and 1.5 arcsecond diameter apertures. The galaxies still appear compact in the averaged images. When we measure the colors of the galaxies in successively larger apertures, they remain constant. There is no evidence for diffuse, redder flux outside of the core. These galaxies have isophotal diameters of ~ 0.5", which corresponds to $\sim 4kpc$ ($H_0 = 65$ km s^{-1} Mpc^{-1}, $q_0 = 0.125$). We measure a 5σ depth at 1.6 microns of AB ≈ 29.8 $\Box''^{-1}$.

4. The Expected Extended Flux from Compact Galaxies

In the previous section we have set approximate empirical limits on the count rate in the H_{160} band through an annuli with inner diameter 0.6" and outer diameter of 1.5" associated with the mean of the isolated U_{300} and B_{450} drop-out galaxies described above. Our failure to detect such extended flux may be interpreted in at least two ways:

1. They are either the bright nuclei or star forming knots in galaxies with lower average surface brightness made up of an older, cooler population (we make no attempt to distinguish between these two possibilities).

2. They are young protogalaxy fragments which are not embedded in an older stellar population.

Colley *et al.* (1996) argue for the former of these two possibilities on the basis of the two-point correlation function, but our sample contains too few objects to make this a decisive test. When we repeat Colley *et al.* analysis we also find a significant signal in the autocorrelation function on small scales, but visual inspection of the images shows that the galaxy pairs responsible for the signal are often obviously two pieces of the same galaxy (Storrie-Lombardi *et al.* 1999). Thus, the distinction between "separate correlated galaxies" and patches of the same galaxy is rather artificial and depends not only on the signal-to-noise ratio of the data but also the parameters used in the source extraction algorithm.

An alternative approach is to ask whether the surrounding lower surface brightness material from the putative older population would be expected to be detectable or not if it were placed at either of the two representative redshifts ($z = 2.7$ and $z = 3.9$) inferred for the U_{300} and B_{450} drop-out subsamples described above. To stay as close to the data set we are analyzing as possible, we selected a relatively bright galaxy from the HDF with a reliable photometric

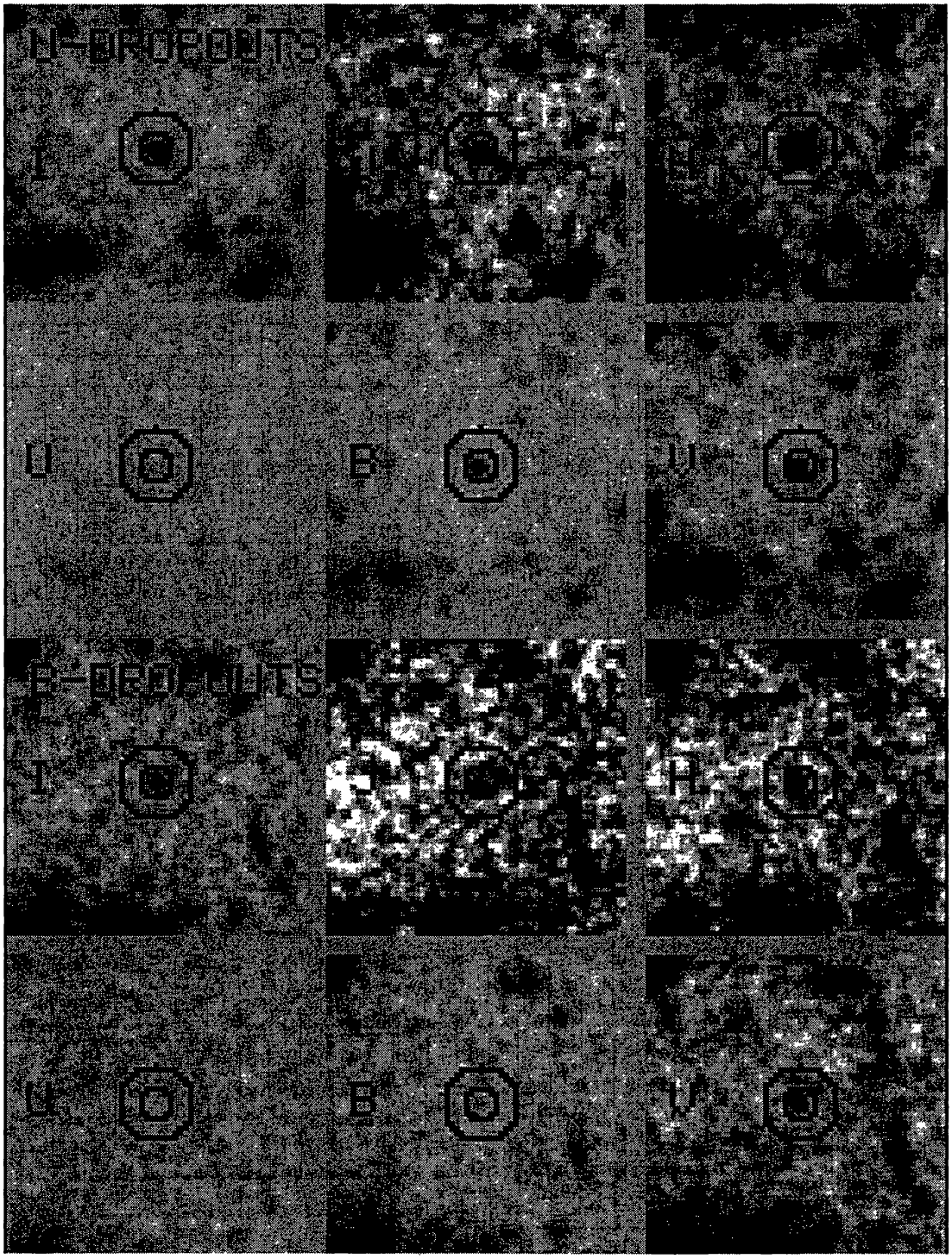

Figure 1. The averaged isolated U_{300} and B_{450} drop-out galaxies are shown in the 6 HST wavebands. The estimated photometric redshifts are $z = 2.70$ and $z = 3.9$, respectively. The frames are 6.0 arcseconds on a side and the averaged galaxies are overlayed with 0.6 and 1.5 arcsecond diameter apertures.

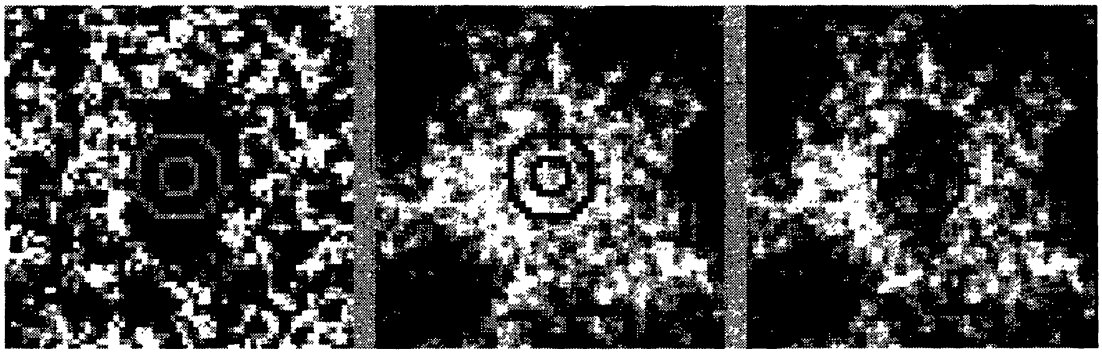

Figure 2. The figure simulates what a starforming galaxy at a redshift of $z \sim 1.15$ would look like in H_{160} if it were redshifted to $z = 3.9$. The left panel shows galaxy HDF 4–378.0, taken from the WFPC2 V_{606} image. The center image shows a region of 'sky' from averaged blank regions in the NICMOS H_{160} image. The right panel shows the blank background with the galaxy scaled to the expected brightness in H_{160} at $z = 3.9$ added to it. Though the full extent of HDF 4–378.0 would not be visible at $z = 3.9$, the resulting galaxy is clearly larger than the 0.6" aperture, in contrast to what we see in our small galaxy sample. All the images are 6 arcseconds on a side and apertures of diameter 0.6 and 1.5 arcseconds are overlayed.

redshift, HDF 4–378.0 at $z = 1.15$. It provides a good example of a galaxy with bright starforming regions surrounded by an older population or less actively starforming regions. The best least squares fit between the observed broadband *annular* fluxes and those calculated on a grid of models in redshift–reddening–population type space for this galaxy is very good and constrains the spectral energy distribution over the range covered from the U_{300} band to the H_{160} band fairly tightly (even though there is ambiguity between, *e.g.*, a very hot, but internally reddened population and a somewhat cooler but unreddened population). With this best fit model, and the observed flux in the bandpasses which most nearly corresponds to the 1.6 micron bandpass if the $z \sim 1$ galaxy were redshifted to the two representative redshifts above, we can calculate the expected flux at higher redshift. (In this calculation we ignore the change in proper length with fixed angle, since over this redshift range this change is very small for most cosmological models.)

Figure 2 shows what HDF 4–378.0 would look like if observed at $z = 3.9$ at 1.6 microns. The left panel shows the undimmed galaxy taken from the WFPC2 V_{606} image. The center image shows a region of 'sky' from averaged blank regions in the NICMOS H_{160} image. The right panel shows the blank background with the galaxy scaled to the expected brightness in H_{160} at $z = 3.9$ added to it. Though the full extent of 4–378.0 would not be visible at $z = 3.9$, it is obvious that the resulting galaxy is larger than the isolated galaxies we have detected, and the flux is easily measurable outside of the 0.6" aperture. The images in the figure are 6 arcseconds on a side and apertures of diameter 0.6 and 1.5 arcseconds are overlayed.

5. Summary and Discussion

Our results suggest that the small, high redshift, galaxies detected in the HDF are bonafide compact objects, not bright nuclei or star forming knots embedded in older, cooler, more extended stellar populations. Our simulations have shown that a prototypical extended galaxy with bright clumps detected easily in the HDF at redshift $z \sim 1$ would still be detected at $z = 3.9$ in the NICMOS observations at 1.6 microns. The small galaxies are consistent with being young protogalaxy fragments. Our photometric redshift estimator prefers the hottest galaxy template (a 50 Myr starburst) with a small amount of reddening for both the U_{300} and B_{450} drop-outs, and gives mean redshifts of $z = 2.7$ and $z = 3.9$ for these, respectively. Numerical simulations by Steinmetz (1998) have shown that the progenitors of a galaxy at $z = 0$ formed in a hierarchical clustering scenario would be detected at $z = 3$ as several protogalactic clumps (Haehnelt, Steinmetz & Rauch 1996) covering an area on the sky the size of a WFPC2 chip or larger. Our results are consistent with this picture.

Acknowledgments. We thank Ron Marzke and Dave Thompson for their useful suggestions.

References

Bertin, E., and Arnouts, S. 1996, A&A, 117, 393

Colley, W.N., Rhoads, J.E., Ostriker, J.P., & Spergel, D.N. 1998, ApJ,473, L63

Ferguson, H.C. 1998, in 'STSCI Symposium: The Hubble Deep Field,' eds. Livio, M., Fall, S.M., Madau, P. (Cambridge University Press:New York), 181

Haehnelt, M., Steinmetz, M. & Rauch, M. 1996, ApJ, L95

Ibata, R., Richer, H., Gilliland, R. & Scott, D., 1999, submitted

O'Connell, R.W.., and Marcum, P. 1997, in proceedings of 'The Hubble Space Telescope and the High Redshift Universe,' eds. Tanvir, N.R., Aragón-Salamanca, A., & Wall, J.V., (World Scientific:London) 63

Steinmetz, M. 1998, in proceedings of 'Space Telescope Science Institute Symposium: The Hubble Deep Field,' eds. Livio, M., Fall, S.M., Madau, P. (Cambridge University Press:New York), 168

Storrie-Lombardi, L.J., Weymann, R.J. & Thompson, R.I. 1999, in preparation

Thompson, R.I., Storrie-Lombardi, L.J., Weymann, R.J., Rieke, M.J, Schneider, G., Stobie, E. & Lytle, D. 1999, AJ, 117, 17

Weymann, R.J., Thompson, R.I. & Storrie-Lombardi, L.J. 1999, ApJ, submitted

Williams, R.E., Blacker, B. Dickinson, M., Dixon, W.V.D, Ferguson, H.C., Fruchter, A.S., Giavalisco, M., Gilliland, R.L., Heyer, I. Katsanis, R., Levay, Z. Lucas, R.A., McElroy, D.B., Petro, L., Postman, M., Adorf, H-M., and Hook, R.N. 1996, AJ, 112, 1335.